

Electroweak Measurements from Hadron Colliders[‡]

Marcel Demarteau

Fermilab
Batavia, IL 60510, USA

Abstract

A review of recent electroweak results from hadron colliders is given. Properties of the W^\pm and Z^0 gauge bosons using final states containing electrons and muons based on large integrated luminosities are presented. The emphasis is placed on the measurement of the mass of the W boson and the measurement of trilinear gauge boson couplings.

[‡]Invited talk given at the *XVI International Workshop on Weak Interactions and Neutrinos*, Capri, Italy, June 22 – 28, 1997.

Electroweak Results from Hadron Colliders

Marcel Demarteau

A review of recent electroweak results from hadron colliders is given. Properties of the W^\pm and Z^0 gauge bosons using final states containing electrons and muons based on large integrated luminosities are presented. The emphasis is placed on the measurement of the mass of the W boson and the measurement of trilinear gauge boson couplings.

1 Introduction

The standard model of electroweak interactions (SM) has taken a very prominent position in today's description of experimental results. Perhaps the most compelling reason for this state of affairs is that the experimental results have reached a level of precision which require a comparison with theory beyond the Born calculations, which the SM is able to provide. It is widely anticipated, though, that the SM is just an approximate theory and should eventually be replaced by a more complete and fundamental description of the underlying forces in nature. Since the highest center of mass energies are reached at hadron colliders, notably the Tevatron, the measurements at this accelerator provide natural tools to probe the SM at the highest energy scale.

In this summary the most recent electroweak results from the multi-purpose detectors CDF and DØ operating at the Fermilab Tevatron $\bar{p}p$ Collider will be described. The DØ detector has a non-magnetic inner tracking system, compact, hermetic, uranium liquid-argon calorimetry and an extensive muon system. The CDF detector has a magnetic central detector, scintillator based calorimetry and a central muon system. During the 1992-1993 run, generally called Run Ia, the CDF and DØ experiments have collected $\sim 20 \text{ pb}^{-1}$ and $\sim 15 \text{ pb}^{-1}$ of data, respectively. For the 1994-1995 run (Run Ib) both experiments have collected $\sim 90 \text{ pb}^{-1}$ of data. First, results on inclusive and differential W and Z production cross sections are presented. The W mass measurement is then described with its dominant uncertainties. In the last section triple gauge boson interactions are discussed.

2 IVB Production Cross Sections

In $\bar{p}p$ collisions intermediate vector bosons are produced predominantly by quark-antiquark annihilation.

At $\sqrt{s} = 1.8 \text{ TeV}$ sea-sea interactions contribute approximately 20% to the total cross section. The leptonic decay modes of the W and Z -bosons are easily detected because of their characteristic decay signatures: for a W decay a high p_T lepton accompanied by large missing transverse energy (\cancel{E}_T), indicating the presence of a neutrino, and two high p_T leptons for Z -decays. The measurement of the W and Z production cross sections probes the SM of electroweak and strong interactions and provides insight in the structure of the proton. A persistent uncertainty on any cross section measurement at a $\bar{p}p$ collider, however, is the large uncertainty on the integrated luminosity due to the uncertainty on the effective total $\bar{p}p$ cross section seen by the detectors. This uncertainty cancels completely in the ratio of the W and Z production cross sections, a quantity that can be used to extract the width of the W -boson, Γ_W . The measurement of the individual cross sections is thus geared towards maximizing the cancellation of the different uncertainties in the ratio of the two cross section measurements.

	DØ		CDF
	e	μ	e
W Candidates	59579	4472	13796
A_W (%)	43.4 ± 1.5	20.1 ± 0.7	34.2 ± 0.8
ϵ_W (%)	70.0 ± 1.2	24.7 ± 1.5	72.0 ± 1.2
Bkg W (%)	8.1 ± 0.9	18.6 ± 2.1	14.1 ± 1.3
$\int \mathcal{L} \text{ (pb}^{-1}\text{)}$	75.9 ± 6.4	32.0 ± 2.7	19.7 ± 0.7
Z Candidates	5702	173	1312
A_Z (%)	34.2 ± 0.5	5.7 ± 0.5	40.9 ± 0.5
ϵ_Z (%)	75.9 ± 1.2	43.2 ± 3.0	69.6 ± 1.7
Bkg Z (%)	4.8 ± 0.5	8.0 ± 2.1	1.6 ± 0.7
$\int \mathcal{L} \text{ (pb}^{-1}\text{)}$	89.1 ± 7.5	32.0 ± 2.7	19.7 ± 0.7

Table 1: Analysis results for the W and Z -production cross section measurement for CDF and preliminary results for DØ. A_V , ϵ_V and Bkg stand for acceptance, detection efficiency and Bkg, respectively, for vector boson V .

The event selection for W -bosons requires an isolated lepton with transverse momentum $p_T >$

25 (20) GeV and $\cancel{E}_T > 25$ (20) GeV for DØ (CDF). Leptonic decays of Z -bosons are selected by imposing the same lepton quality and kinematic cuts on one lepton, and looser requirements on the second lepton. Table 1 lists the kinematic and geometric acceptance (A_V), trigger and event selection efficiency (ϵ_V) and background (Bkg) for the electron and muon decay channel for the two experiments ($V = W/Z$) [1].

	$\sigma_W \cdot B(W \rightarrow \ell\nu)$	$\sigma_Z \cdot B(Z \rightarrow \ell\ell)$
DØ (e)	$2.38 \pm 0.01 \pm 0.22$	$0.235 \pm 0.003 \pm 0.021$
DØ (μ)	$2.28 \pm 0.04 \pm 0.25$	$0.202 \pm 0.016 \pm 0.026$
CDF (e)	$2.49 \pm 0.02 \pm 0.12$	$0.231 \pm 0.006 \pm 0.011$

Table 2: Preliminary DØ results on the measured cross section times branching ratio in nb for W and Z production from the 1994-1995 run based on an integrated luminosity of 89.1 (32.0) pb^{-1} for the electron (muon) decay, and published CDF results from the 1992-1993 data based on an integrated luminosity of 19.7 pb^{-1} .

The vector boson inclusive cross section times decay branching ratio follows from the number of background subtracted observed candidate events, corrected for efficiency, acceptance and luminosity: $\sigma \cdot B = \frac{N_{obs} - N_{bkg}}{A \epsilon \mathcal{L}}$, where N_{obs} is the observed number of events and N_{bkg} the number of expected background events. B indicates the branching ratio of the vector boson for the decay channel under study. The measured cross sections times branching ratio are listed in Table 2 and are compared with the theoretical prediction in Fig. 1. The theoretical predictions for the total production cross section, calculated to $\mathcal{O}(\alpha_s^2)$ [2], depend on three input parameters: the mass of the W -boson, M_W , the mass of the Z -boson, M_Z , and the structure of the proton. Using the CTEQ2M parton distribution functions [3], the predictions for the total cross sections are $\sigma_W = 22.35$ nb and $\sigma_Z = 6.708$ nb. Using the leptonic branching ratio $B(W \rightarrow \ell\nu) = (10.84 \pm 0.02)\%$, as calculated following reference [4] using $B(Z \rightarrow \ell\ell) = (3.366 \pm 0.006)\%$ as measured by the LEP experiments [5], the theoretical predictions for the total inclusive production cross section times branching ratio are $\sigma_W \cdot B(W \rightarrow \ell\nu) = 2.42_{-0.11}^{+0.13}$ nb and $\sigma_W \cdot B(Z \rightarrow \ell\ell) = 0.226_{-0.009}^{+0.011}$ nb. The two largest uncertainties on the theoretical prediction are the choice of parton distribution function (pdf) (4.5%) and the uncertainty due to using a NLO parton

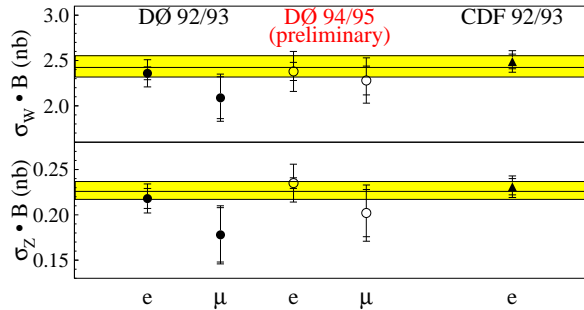


Figure 1: Measurements of the W and Z inclusive cross section compared with the theoretical prediction using the CTEQ2M parton distribution function. The shaded bands indicate the uncertainty on the predictions.

distribution function with a full $\mathcal{O}(\alpha_s^2)$ theoretical calculation (3%). The pdf uncertainty is not expected to decrease as rapidly as the statistical error on the measurement. The experimental error is dominated by the uncertainty on the luminosity. At the moment this uncertainty seems irreducible. Since there is good agreement between the theoretical prediction and the observed cross section it may therefore become advantageous to measure the luminosity using the observed W event rate.

The ratio of the cross section measurements in which the error on the luminosity, common to both the W and Z events, completely cancels measures the leptonic branching ratio of the W -boson. It can be used, within the framework of the SM, to extract the total width of the W -boson:

$$R = \frac{\sigma_W \cdot B(W \rightarrow \ell\nu)}{\sigma_Z \cdot B(Z \rightarrow \ell\ell)} = \frac{\sigma_W}{\sigma_Z} \cdot \frac{\Gamma(W \rightarrow \ell\nu)}{\Gamma(Z \rightarrow \ell\ell)} \frac{\Gamma(Z)}{\Gamma(W)}$$

which gives

$$B^{-1}(W \rightarrow \ell\nu) = \frac{\sigma_W}{\sigma_Z} \cdot \frac{1}{B(Z \rightarrow \ell\ell)} \cdot \frac{1}{R}.$$

Using the SM prediction for the partial decay width $\Gamma(W \rightarrow \ell\nu)$ [4], the total decay width of the W , Γ_W , is given by

$$\Gamma_W = \frac{\sigma_W}{\sigma_Z} \cdot \frac{\Gamma(W \rightarrow \ell\nu)}{B(Z \rightarrow \ell\ell)} \cdot \frac{1}{R}.$$

The ratio of the cross sections, using the calculation of [2], is determined to be 3.33 ± 0.03 . Even though in the ratio the theoretical uncertainties also largely cancel, the error is still dominated by the choice of pdf's. Using, as before, the measured branching ratio $B(Z \rightarrow \ell\ell) =$

$(3.367 \pm 0.006)\%$ and the theoretical prediction for the partial decay width $\Gamma(W \rightarrow \ell\nu) = 225.2 \pm 1.5$ MeV [4] the W leptonic branching ratio, as determined from the combined $D\bar{O}$ electron and muon 1992-1993 data, is $(10.43 \pm 0.44)\%$; the CDF measured branching ratio, based on the 1992-1993 electron data is $(10.94 \pm 0.33 \pm 0.31)\%$. Using the calculated partial leptonic branching ratio of the W , these measurements yield for the width $\Gamma_W = 2.159 \pm 0.092$ GeV and $\Gamma_W = 2.043 \pm 0.082$ GeV [1], respectively. The CDF value differs from their published value due to the use of more recent experimental measurements in evaluating the input parameters. Figure 2 shows the world W -width measurements together with the theoretical prediction [1, 6, 7, 8, 9].

Taking into account that the ratio of the total cross sections σ_W/σ_Z is slightly different at a center of mass energy of 630 GeV ($\sigma_W/\sigma_Z(\sqrt{s} = 630$ GeV) = 3.26 ± 0.09), and accounting for the correlation between the measurements at different center of mass energies through the choice of pdf's, the different values of Γ_W can be combined to give a world average of $\Gamma_W = 2.062 \pm 0.059$ GeV, a measurement at the 3% level. This is in good agreement with the SM prediction of $\Gamma(W) = 2.077 \pm 0.014$ GeV. The comparison of the measurement with the theoretical prediction can be used to set an upper limit on an “excess width” $\Delta\Gamma_W \equiv \Gamma_W(\text{meas}) - \Gamma_W(\text{SM})$, allowed by experiment for non-SM decay processes, such as decays into supersymmetric particles or into heavy quarks. Comparing the above world average value of Γ_W with the SM prediction a 95% C.L. upper limit of $\Delta\Gamma_W < 109$ MeV on unexpected decays can be set.

3 Drell-Yan Production

One of the unique features of $\bar{p}p$ collisions is the intrinsic large range of available partonic center of mass energies. This allows for a study of the Z line shape through the Drell-Yan process ($q\bar{q} \rightarrow (\gamma, Z) \rightarrow \ell^+\ell^-$) over a large di-lepton invariant mass region. The low invariant mass region allows access to the small x region of the parton distribution functions down to $x = 0.006$, where x is the fraction of the proton momentum carried by the parton. The high invariant mass region is populated by high x partons and thus allows for a study of a possible substructure of the interacting

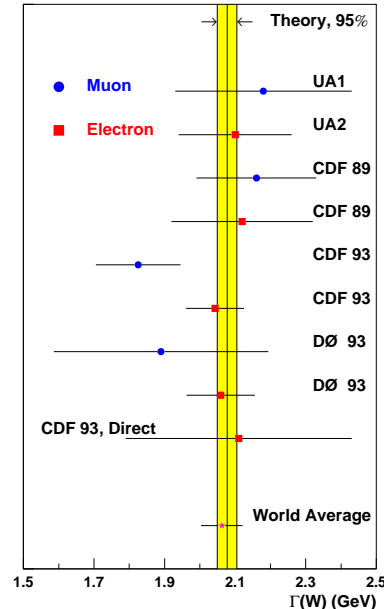


Figure 2: Measurements of Γ_W compared with the SM expectation.

partons. A possible substructure would manifest itself most prominently in a modification of the γZ interference pattern whose effects are strongest in the region well above the Z pole. Substructure of partons is most commonly parametrized in terms of a contact interaction [10],

$$\mathcal{L} = \mathcal{L}_{\text{SM}} + \eta \frac{g_0^2}{\Lambda_{ij}^2} (\bar{\psi}_i \gamma^\mu \psi_i) (\bar{\psi}_j \gamma^\mu \psi_j) \quad (1)$$

characterized by a phase, η , leading to constructive ($\eta = -1$) or destructive interference ($\eta = +1$) with the SM Lagrangian, and a compositeness scale, Λ_η , indicative of the energy scale at which substructure would be revealed. The indices i, j refer to the chirality of the interacting fermions. The coupling constant g_0^2 is taken to be 4π . By fitting the di-lepton invariant mass spectrum to various assumptions for the compositeness scale, phase of the interference and chirality of the interaction, lower limits on the compositeness scale can be set.

The CDF experiment has measured the double differential Drell-Yan cross section $d^2\sigma/dM dy$ for electron and muon pairs in the mass range

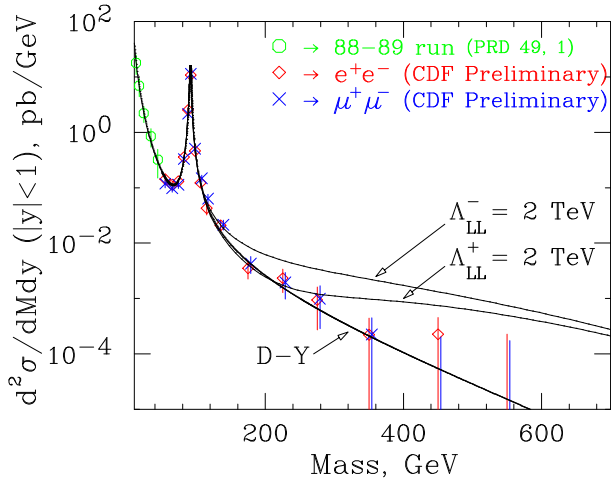


Figure 3: Double differential cross section $d^2\sigma/dM dy$ for CDF electron and muon data combined. The open symbols are from the 88–89 data. The solid symbols correspond to the full Run I data. The curves are the theoretical predictions for a lefthanded-lefthanded contact interaction with a scale of 2 TeV for constructive and destructive interference.

$11 < M_{\ell\ell} < 150 \text{ GeV}/c^2$ for the Run Ia data [11], and $40 < M_{\ell\ell} < 550 \text{ GeV}/c^2$ for the Run Ib data [12]. The di-electron invariant mass spectrum is measured over the rapidity interval $|\eta| < 1$. Due to a more restricted coverage, the muon cross section has been determined only over the range $|\eta| < 0.6$. Figure 3 shows the measured cross section for electrons and muons combined. The curves correspond to a leading-order calculation of the Drell-Yan cross section with in addition a contact interaction between the quarks and leptons. The theoretical predictions have been normalized to the data over the Z resonance region of $50 < M < 150 \text{ GeV}/c^2$, which removes the uncertainty due to the luminosity and reduces the effect of the systematic uncertainty on the acceptance. Performing a maximum likelihood fit to the electron and muon data combined of Monte Carlo generated spectra for different assumptions for the contact interaction, scale factors are obtained as listed in Table 3. The limits imply that up to a distance of 10^{-17} cm the interacting particles reveal no substructure. The limits from other experiments on quark-lepton contact interactions are slightly less stringent. The lower limits range from 1.6 - 2.5 TeV from LEP [13], and 1.0 - 2.5 TeV from HERA [14].

The distribution shown in Fig. 3 can be di-

Model	LL	LR	RL	RR	VV	AA	SC
Λ^+	3.1	3.3	3.3	3.0	5.0	4.5	3.3
Λ^-	4.3	3.9	3.7	4.2	6.3	5.6	3.3

Table 3: One-sided 95% confidence level lower limits on the compositeness scale (in TeV) for different chiralities of the contact interaction and different phases of interference with the SM Lagrangian.

vided into two invariant mass regions: a pole region, $75 < M_{\ell\ell} < 105 \text{ GeV}/c^2$ and a high mass region with $M_{\ell\ell} > 105 \text{ GeV}/c^2$ and the forward backward asymmetry, A_{FB} , can be measured for those two regions. A_{FB} is defined as $A_{FB} = \frac{\sigma_F - \sigma_B}{\sigma_F + \sigma_B}$ where $\sigma_{F(B)}$ is the cross section for fermion production in the forward (backward) hemisphere. Because the left-handed and right-handed coupling of fermions to the Z boson are not the same, the angular distribution of the outgoing fermion with respect to the incoming fermion in the parton center of mass frame exhibits a forward-backward asymmetry. Due to the changing polarization of the Z boson as function of center of mass energy A_{FB} has a strong energy dependence, which can be measured by studying A_{FB} in different di-lepton invariant mass regions.

Since the couplings of the fermions to the Z boson depend on the fermion weak isospin and charge, A_{FB} is different for different initial and final states. For the Drell-Yan process $\bar{p}p \rightarrow \ell^+\ell^-$ no distinction can be made between $u\bar{u}$ and $d\bar{d}$ initial states and therefore the asymmetry measured will be a convolution of both. It is interesting to note that this process is the time-reversal of the corresponding process at e^+e^- -machines and the measurements are complementary. At LEP and SLC the measurements are free from pdf uncertainties, whereas at the Tevatron, the light quark asymmetries are free from fragmentation uncertainties.

The CDF experiment has measured A_{FB} using the full Run I data set for di-electron final states with $|\eta_{\ell_1}| < 1.1$ and $|\eta_{\ell_2}| < 2.4$ [15]. The analysis yields $A_{FB} = 0.07 \pm 0.016$ for $75 < M_{ee} < 105 \text{ GeV}/c^2$, and $A_{FB} = 0.43 \pm 0.10$ for $M_{ee} > 105 \text{ GeV}/c^2$, compared to the SM predictions of $A_{FB} = 0.054 \pm 0.001$ and $A_{FB} = 0.528 \pm 0.006$, respectively. Even though in the high mass region the asymmetry is measured with a rather large error, these measurements still serve as a probe of extensions of the SM because models with ad-

ditional heavy neutral gauge bosons can substantially alter A_{FB} [16]

4 W -mass

A possible choice of the fundamental parameters of the gauge sector of the standard model of electroweak interactions is the fine structure constant, α , the Fermi constant, G_F and the mass of the Z boson, M_Z , all measured to very high precision. Within the SM the mass of the W boson is then predicted and can be expressed in terms of these parameters. In the on-shell scheme the mass of the W boson is given by

$$M_W^2 = \frac{M_Z^2}{2} \left(1 + \sqrt{1 - \frac{4\pi\alpha}{\sqrt{2}G_\mu M_Z^2} \frac{1}{1 - \Delta r}} \right) \quad (2)$$

where Δr measures the higher order corrections. That is, at tree level Δr vanishes. The dominant contribution to Δr comes from the photon vacuum polarization which contributes about 0.06 to Δr . The other contributions come from the vector boson self-energies, the top quark which introduces a dependence quadratic in M_t and the Higgs boson, which adds a dependence logarithmic in M_H . Of course, also new physics would contribute to Δr . A precise measurement of the W boson mass is thus a direct measure of the radiative corrections in the SM and combined with the measurement of M_t it forms a constraint on the Higgs mass if the measurements are precise enough. In addition it is sensitive to physics not included in the minimal SM.

In W events produced in hadronic collisions in essence only two quantities are measured: the lepton momentum and the transverse momentum of the recoil system. The latter consists of the “hard” W -recoil and the azimuthally symmetric underlying event contribution. It should be noted that the underlying event contribution is luminosity dependent. The neutrino transverse momentum is equated to the total missing transverse energy in the event, \vec{E}_T^{miss} . Since the longitudinal momentum of the neutrino cannot be determined unambiguously, the W -boson mass is determined from the line shape in transverse mass, defined as

$$m_T = \sqrt{2 p_T^\ell p_T^\nu (1 - \cos \varphi^{\ell\nu})}. \quad (3)$$

Here $\varphi^{\ell\nu}$ is the angle between the lepton and neutrino in the transverse plane. Since there is no analytic description of the transverse mass distribution, the W -mass is determined by fitting Monte Carlo generated templates in transverse mass for different masses of the W -boson to the data. The distribution in m_T exhibits a Jacobian edge characteristic of two-body decays which contains most of the mass information. For the W -mass determination both the energy scale for the lepton and recoil system, which determine the peak position of the transverse mass distribution, as well as the resolution on the measured variables, which controls the steepness of the Jacobian edge, are crucial.

Both the CDF and DØ mass analyses discussed here are based on the Run Ib data, with the CDF analysis based on W decays into muons and the DØ analysis based on electrons. In the CDF W -mass analysis the momentum scale of the central magnetic tracker is set by scaling the measured J/ψ -mass to the world average value using $J/\psi \rightarrow \mu^+ \mu^-$ decays. Based on a sample of approximately 250,000 events the ratio of the measured and true J/ψ mass has been determined to be 0.99977 ± 0.00048 . The dominant contribution to the uncertainty on the momentum scale at the J/ψ mass comes from the uncertainty in the amount of material the muons traverse. To establish the momentum scale at the W -mass the measured J/ψ -mass is studied as function of $\langle 1/p_T^2 \rangle$, extrapolated to zero curvature and verified with measurements of the Z and Υ resonances. Figure 4 shows the measured momentum scale factor with its uncertainty as function of mass. The hatched region indicates the error incurred by extrapolating the momentum to the momentum scale appropriate for muons from W decays. Also shown are ratios of the measured mass and world average mass for various other resonances. The measurements agree well, within the statistical uncertainty, with the scale determined from the J/ψ mass. An overall uncertainty of 0.00048 on the momentum scale has been determined resulting in a 40 MeV/ c^2 uncertainty on the W mass.

At DØ the W -mass is measured from $W \rightarrow e\nu$ decays. The electromagnetic (EM) energy scale is determined by calibrating to the $Z \rightarrow ee$ resonance in conjunction with the reconstruction of π^0 and J/ψ decays. Since the absolute energy scale of the EM calorimeter is not known with the pre-

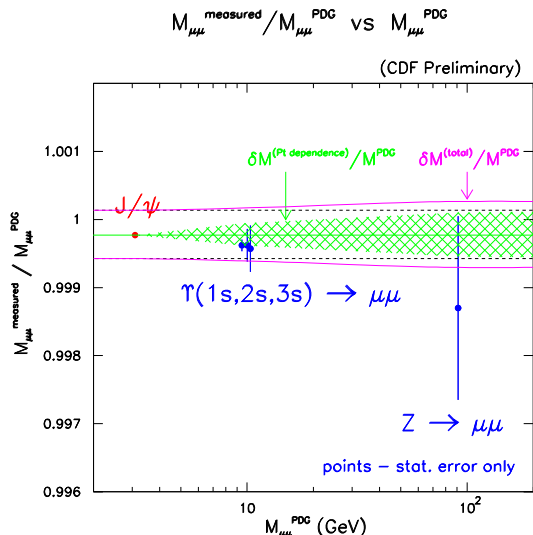


Figure 4: Ratio of measured and world average mass for various resonances. The dotted line indicates the total uncertainty on the momentum scale.

cision required for this measurement, in essence the ratio of the W and Z masses is measured, anchored to the LEP Z mass.

To establish the energy scale it is necessary to determine to which extent a potential offset in the energy response, as opposed to a scale factor, is responsible for the deviation of the ratio $\frac{M_W^{D\phi}}{M_Z^{LEP}}$ from unity. This was achieved by combining the measured Z mass with the measurements of $\pi^0 \rightarrow \gamma\gamma$ and $J/\psi \rightarrow e^+e^-$ decays and comparing them to their known values. If the electron energy measured in the calorimeter and its true energy are related by $E_{\text{meas}} = \alpha E_{\text{true}} + \delta$, the measured and true mass values are, to first order, related by $m_{\text{meas}} = \alpha m_{\text{true}} + \delta f$. The variable f depends on the decay topology and is given by $f = \frac{2(E_1 + E_2)}{m_{\text{meas}}} \sin^2 \gamma/2$, where γ is the opening angle between the two decay products and E_1 and E_2 are their measured energies. The ratio of the measured W and Z mass in this approximation can then be written as

$$\frac{M_W(\alpha, \delta)}{M_Z(\alpha, \delta)} \Big|_{\text{meas}} = \frac{M_W}{M_Z} \Big|_{\text{true}} \left[1 + \frac{\delta}{\alpha} \cdot \frac{f_W M_Z - f_Z M_W}{M_Z \cdot M_W} \right].$$

It should be noted that the W mass is insensitive

to α if $\delta = 0$ and that the sensitivity to δ is proportional to f . Decays with different values for f will thus have different sensitivity to the offset δ . By combining the $Z \rightarrow ee$, $\pi^0 \rightarrow \gamma\gamma \rightarrow eeee$ and $J/\psi \rightarrow ee$ analysis, this in situ calibration of the EM calorimeter yields $\alpha = 0.95329 \pm 0.00077$ and $\delta = (-0.160 \pm 0.016^{+0.060}_{-0.210})$ GeV. The asymmetric error on the offset is largely due to possible calorimeter nonlinearities, which is dominated by the uncertainty on the low energy response of the calorimeter. This uncertainty on the absolute energy scale results, for the Run Ib data sample, in an uncertainty on M_W of 70 MeV/ c^2 , of which 65 MeV/ c^2 is due to the limited Z statistics.

After the energy scale has been set, the W -mass is determined from a maximum likelihood fit of Monte Carlo generated templates in transverse mass to the data distribution. In the Monte Carlo model of W -production the triple differential production cross section is assumed to factorize into a term describing the mass dependence of the cross section and a term describing the longitudinal and transverse motion of the boson. The mass dependence is taken to be a relativistic Breit-Wigner resonance, adjusted for parton luminosity effects. The distribution in p_T and rapidity of the W boson is modeled according to the parametrization by Ladinsky and Yuan [17] with a particular choice for pdf, thus including the correlation between the longitudinal and transverse momentum. The CDF choice for nominal pdf is the MRS R2- pdf [18], whereas D ϕ uses the MRSA pdf [19]. After the W bosons are generated the decay is modeled, respecting the polarization of the boson [20].

The decay products are then traced through the detector and the detector response simulated. The parameters of the detector model are constrained by the data itself. The width of the Z -resonance, for example, provides a constraint on the momentum and energy resolution. The calorimeter response to the recoil of the W boson is also determined using Z events, by comparing the p_T of the Z obtained from the two electrons, \vec{p}_T^{ee} , to that obtained from the rest of the event, \vec{p}_T^{ec} . If the response of the hadronic calorimeter were equal to the response of the EM calorimeter the vector sum of these two different measures of p_T^Z would on average be zero. To minimize the contribution from the electron energy resolution, the vector sum of these two quantities is projected along the bisector of the two electron directions,

called the η -axis. By studying $\vec{p}_T^{ee} + \vec{p}_T^{rec}$ as function of \vec{p}_T^{ee} the relative response of the hadronic calorimeter with respect to the electromagnetic calorimeter is determined. Figure 5 shows for the CDF experiment the quantity δ defined through the relation $|\vec{p}_T^{rec}| = (1 - \delta)|\vec{p}_T^{ee}|$, as function of $\vec{p}_T^{ee} \cdot \hat{\eta}$. It can be seen that the CDF hadronic response is about 45% lower than the electromagnetic response.

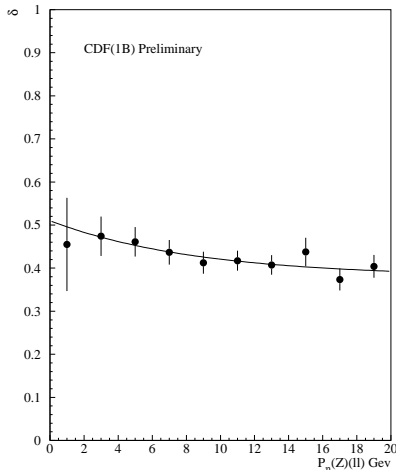


Figure 5: Deviation of the hadronic response relative to the electromagnetic response of the CDF calorimeter as function of \vec{p}_T^{ee} projected onto the bi-sector of the two electron directions.

Both experiments model the underlying event using minimum bias data, mimicking the debris in the event due to spectator parton interactions and the pile-up associated with multiple interactions, and including the residual energy from previous beam crossings.

The mass of the W is obtained from a maximum likelihood fit in m_T of events in the transverse mass range $65 < m_T < 100 \text{ GeV}/c^2$ ($60 < m_T < 90 \text{ GeV}/c^2$) for CDF (DØ) to a data sample obtained by applying very stringent fiducial and kinematic cuts. Both experiments use only central leptons to determine the W mass. Figure 6 shows the transverse mass distributions for the data together with the best fit of the Monte Carlo for the Run Ib muon data for CDF. The W -mass is determined to be $M_W^e = 80.450 \pm 0.070(\text{stat.}) \pm 0.095(\text{syst.}) \text{ GeV}/c^2$ by DØ and $M_W^\mu = 80.430 \pm 0.100(\text{stat.}) \pm 0.120(\text{syst.}) \text{ GeV}/c^2$

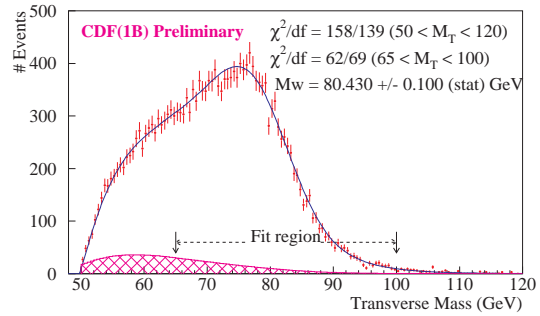


Figure 6: CDF transverse mass distribution of $W \rightarrow \mu\nu$ decays collected during the 1994-1995 run. The points are the data and the line is the best fit. The arrows indicate the fit region.

by CDF. Table 4 lists the systematic errors on the individual measurements.

Source	CDF	DØ
	μ	e
Statistical	100	70
Energy/Momentum scale	40	70
Other Systematics	115	70
Lepton Angle	—	30
e or μ resolution	25	25
Recoil Model	90	40
p_T^W Model, pdf's	50	25
QCD/QED corr's	30	20
W -width	—	10
Backgrounds/bias	30	10
Fitting procedure	10	5
Total	155	120

Table 4: Errors on M_W in MeV/c^2 .

Combining these measurements with previous W mass measurements [21], with a conservative assumption of a $50 \text{ MeV}/c^2$ correlated uncertainty due to the parton distribution functions and the input p_T^W spectrum, gives a world average of $M_W = 80.410 \pm 0.090 \text{ GeV}/c^2$ from the $\bar{p}p$ collider experiments. Figure 7 summarizes the current status of the $\bar{p}p$ measurements.

The expectation is that the theoretical uncertainties can be further constrained with a full analysis of the Run I data. The uncertainty due to the pdf's can be constrained using the CDF measured W charge asymmetry in conjunction with the world's data. The W charge asymmetry is de-

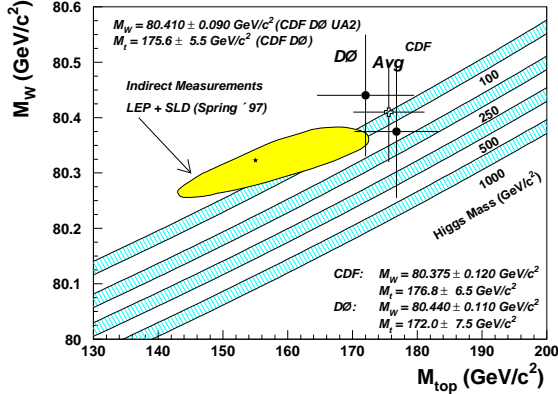


Figure 7: Relation between M_W and M_t in the SM for different values of M_H together with the current direct and indirect measurements of M_W and the measurements of M_t .

defined as

$$A(y_\ell) = \frac{dN^+(y_\ell)/dy_\ell - dN^-(y_\ell)/dy_\ell}{dN^+(y_\ell)/dy_\ell + dN^-(y_\ell)/dy_\ell}$$

where $N^{+(-)}$ is the number of positively (negatively) charged leptons from the W decay detected at pseudorapidity y_ℓ . The rapidity distribution of the decay lepton is governed by both the $V - A$ structure of the W decay and the longitudinal momentum distribution of the W bosons. Since the $V - A$ structure of the W -decay is very well understood, the charge asymmetry measurement can then be used to probe the structure of the proton in the x range 0.007 to 0.27.

CDF has updated the W charge asymmetry measurement using the full Run I data set with a total integrated luminosity of 110 pb^{-1} . In addition, in the new analysis the rapidity coverage for muons has been extended by utilizing the forward muon toroids covering $1.95 < |\eta| < 3.6$, which collected 72 pb^{-1} of data. The efficiency for electrons in the plug calorimeter ($1.1 < |\eta| < 2.4$) was also substantially improved. The agreement between theory and experiment is quantified through the use of a significance parameter defined as

$$\Delta A = \frac{\bar{A}_{pdf} - \bar{A}_{data}}{\sigma(\bar{A}_{data})} \quad (4)$$

where \bar{A} is the weighted mean asymmetry as measured, or as predicted by the DYRAD NLO Monte

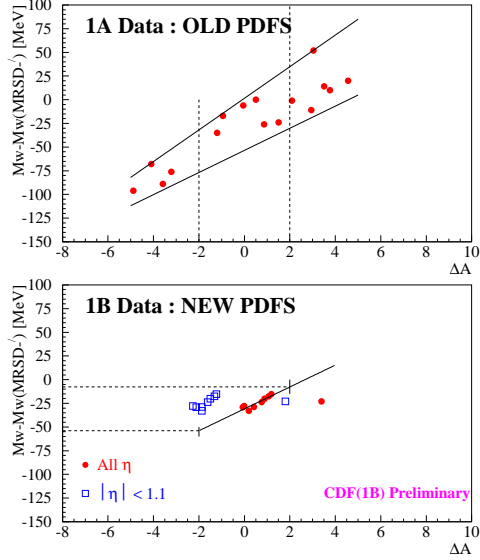


Figure 8: Change in W mass versus significance of deviation between measured and predicted W charge asymmetry for “old” (top) and “new” (bottom) pdf’s.

Carlo [22] using a particular set of pdf’s. The top graph in Fig. 8 shows the variation in M_W versus ΔA for various “old” pdf’s. Here “old” indicates pdf’s determined without inclusion of the CDF Run Ia W charge asymmetry measurement [23]. The label “new” refers to pdf’s which do include that measurement in their determination of the structure functions. One anticipates a further reduction of the $25 \text{ MeV}/c^2$ uncertainty currently assigned due to the pdf uncertainty when the final W charge asymmetry data is included in the global parton distribution fits.

As a conservative estimate, currently also the uncertainty due to the input p_T spectrum is taken as correlated between the two experiments. The W boson mass is extracted from events with low vector boson p_T , a region dominated by soft gluon emission. The soft gluon resummation formalism which describes this region contains a non-perturbative function parametrized in terms of phenomenological parameters, whose values have been derived from fits to Drell-Yan data. It is expected that the measured p_T^Z spectrum will further constrain these parameters and thus the uncertainty due to the W production model.

The $\bar{p}p$ average for M_W can be combined

with the LEP average of $M_W = 80.48 \pm 0.14$ GeV/c², the average of four measurements at both $\sqrt{s} = 162$ and 172 GeV [24], and yields an average, assuming no correlation between the $\bar{p}p$ and e^+e^- measurements, of $M_W = 80.430 \pm 0.080$ GeV/c². The sensitivities of M_W and M_t to $\ln(M_H)$ are $\frac{\partial M_W}{\partial \ln(M_H)} \approx -75$ MeV and $\frac{\partial M_t}{\partial \ln(M_H)} \approx 12$ GeV per unit in $\ln(M_H)$. Given the current measurements with their uncertainties, reducing the uncertainty on M_W by a factor of 2 has about twice the power of an equivalent reduction of the top mass uncertainty.

Looking at Fig. 7 the standard observation is that the measurements agree with the SM. Although such a statement is of course correct, it does not really highlight the enormous achievement of these measurements of the W mass. Recall that Δr is a measurable quantity. The $\bar{p}p$ measurements alone of M_W yield $\Delta r = 0.0335 \pm 0.0054$. That is, Δr is measured with a significance of 6.2σ from its tree level prediction. But, it is well known that Δr is dominated by QED corrections. Following ref. [25] the real electroweak bosonic corrections can be separated out by defining a Δr_{res} :

$$\frac{\alpha}{1 - \Delta r} = \frac{\alpha(M_Z^2)}{1 - \Delta r_{res}}, \quad (5)$$

where the pure QED corrections are absorbed in the running of α . Using again the $\bar{p}p$ measurement of M_W alone one finds $\Delta r_{res} = -0.0276 \pm 0.0059$, a significance from the tree level prediction of 4.8σ , a clear demonstration of weak bosonic corrections in the Standard Model. Including the LEP M_W increases the significance to 5.5σ .

An indirect measurement of the W -mass, through the measurement of the weak mixing angle $\sin^2 \vartheta_W$, is described in detail in the contribution following this one [26].

5 Gauge Boson Pair Production

The non-Abelian $SU(2) \times U(1)$ gauge symmetry of the SM implies that the gauge bosons self-interact. These self-interactions give rise to very subtle interference effects in the SM. In fact, in the SM the couplings are uniquely determined by the gauge symmetry in order to preserve unitarity. An accurate measurement of the gauge boson self-interactions would constitute a stringent test

of the gauge sector of the SM and any observed deviation of the couplings from their SM value would indicate new physics.

The formalism of effective Lagrangians is used to describe gauge boson interactions beyond the SM. The most general effective electroweak Lagrangian contains 2×7 free parameters [27]: $g_1^V, \kappa_V, \lambda_V, g_4^V, g_5^V, \tilde{\kappa}_V, \tilde{\lambda}_V$, with $V = \gamma, Z$. The parameter g_5^V , violates \mathcal{C} and \mathcal{P} but conserves \mathcal{CP} ; $g_4^V, \tilde{\kappa}_V$ and $\tilde{\lambda}_V$ violate \mathcal{CP} . In the SM $g_1^V = 1, \kappa_V = 1$, and all other parameters vanish. For these two parameters one therefore introduces deviations from the SM values, $\Delta\kappa_V = \kappa_V - 1$ and $\Delta g_1^V = g_1^V - 1$.

Gauge boson self-interactions can be studied through di-boson production. The cross sections for di-boson production are generally rather small and a study of the full fourteen-dimensional parameter space is impossible. In general, two approaches are followed to reduce the parameter space. The $\bar{p}p$ experiments generally set all parameters but two to their SM values and concentrate on $\Delta\kappa_V, \lambda_V$ because they have a direct physical connection through the magnetic dipole and electric quadrupole moment of the W boson, $\mu_W = (e/2m_W)(1 + \kappa_\gamma + \lambda_\gamma)$ and $Q_W^e = (-e/m_W^2)(\kappa_\gamma - \lambda_\gamma)$ [28].

The second approach, followed mainly by the LEP experiments, constructs an effective Lagrangian with operators of higher dimension. By imposing some restriction, like retaining only the lowest dimension operators, respecting \mathcal{C}, \mathcal{P} and \mathcal{CP} invariance and requiring the Lagrangian to be invariant under $SU(2) \times U(1)$ and adding a Higgs doublet, the number of free parameters is reduced to just three [29]. With further, rather ad hoc, requirements the parameter space can be reduced to just two free parameters [30], with definite relations between the different parameters [31].

If in the processes of di-boson production the couplings deviate even modestly from their SM values, the gauge cancellations are destroyed and a large increase of the cross section is observed. Moreover, the differential distributions will be modified. A WWV interaction Lagrangian with constant anomalous couplings would thus violate unitarity at high energies and therefore the coupling parameters are modified to include form factors [32], that is, $\Delta\kappa(\hat{s}) = \Delta\kappa/(1 + \hat{s}/\Lambda^2)^2$ and $\lambda(\hat{s}) = \lambda/(1 + \hat{s}/\Lambda^2)^2$, where \hat{s} is the square of the

center of mass energy of the subprocess. Λ is a unitarity preserving form factor scale and indicates the scale at which new physics would manifest itself. Limits on anomalous couplings are therefore always quoted for a particular value of Λ . In the next subsections some gauge boson pair production processes will be discussed.

5.1 $WW \rightarrow \ell\ell'\nu\nu'$ Production

Both the CDF and DØ experiment have searched for W -boson pair production $\bar{p}p \rightarrow WW + X \rightarrow \ell\ell'\nu\nu'$ ($\ell\ell' = ee/e\mu/\mu\mu$) based on data samples with an integrated luminosity of 108 and 97 pb⁻¹, respectively. The very few $t\bar{t}$ events recorded at the Tevatron are a background to this process, removed through cuts on the hadronic activity in the event. Both experiments observe 5 events over a background of 3.3 ± 0.4 and 1.2 ± 0.3 events for DØ and CDF, respectively. This yields for CDF a measurement of the cross section for W -pair production of $\sigma = 10.2_{-5.1}^{+6.3} \pm 1.6$ pb, to be compared to the SM prediction of $\sigma_{SM} = 9.5 \pm 2.9$ pb [33]. It should be noted that the smallness of the cross section in itself is a beautiful demonstration of the gauge cancellations in the SM.

Since anomalous couplings not only result in an increase of the cross section but also significantly alter the differential distributions, limits on anomalous coupling parameters can be set by either using the event rate or by performing a fit to a differential distribution, generally taken to be the p_T of one of the final state particles. Adopting the former approach, CDF has obtained the limits $-1.1 < \Delta\kappa < 1.3$ ($\lambda = 0$) and $-0.8 < \lambda < 0.9$ ($\Delta\kappa = 0$) for $\Lambda = 1.0$ TeV. Performing a two-dimensional fit to the lepton p_T spectra, DØ obtained the limits $-0.62 < \Delta\kappa < 0.75$ ($\lambda = 0$) and $-0.50 < \lambda < 0.56$ ($\Delta\kappa = 0$) for $\Lambda = 1.5$ TeV. Both sets of limits are obtained assuming $\Delta\kappa \equiv \Delta\kappa_\gamma = \Delta\kappa_Z$ and $\lambda \equiv \lambda_\gamma = \lambda_Z$.

5.2 WW and WZ Production

Searches for particle production requiring two leptons in the final state always suffer in event rate due to the small leptonic branching ratios. When in the analysis described in the previous subsection only one lepton is required, a substantial increase in event rate is obtained, though at the cost of a much larger background. The back-

ground from W/Z +jet production to these processes is about 30 times higher than the signal production. Given the distinct characteristics of anomalous couplings this background can be dealt with. Anomalous couplings modify the differential distributions dramatically, especially the transverse momentum distribution of the W -boson. By requiring the vector boson to have high transverse momentum the background is completely eliminated and a good sensitivity to anomalous couplings is retained. One completely loses sensitivity, however, to SM W -pair production.

Both CDF and DØ have looked for W -pair production using the leptonic decay of one of the W bosons and the hadronic decay of the other [34, 35]. Due to the limited jet energy resolution no distinction can be made between WW and WZ production and this analysis is thus sensitive to both processes. The jets from the hadronic decay of the W or Z boson are required to have an invariant mass consistent with the gauge boson mass, $60 < m_{jj} < 110$ GeV/c². Since no distinction can be made between WW and WZ -production in this selection, CDF has increased the sensitivity of the study by including $\bar{p}p \rightarrow WZ \rightarrow q\bar{q}'\ell\ell$ events, requiring the di-lepton invariant mass to reconstruct to the Z -boson mass.

Limits on anomalous couplings have been set by comparing the measured p_T^W spectrum with the expectation using either the rate of events with $p_T^W > 200$ GeV/c, using both the electron and muon decays of W 's (CDF) or by performing a maximum likelihood fit to the full differential distribution in p_T^W for W decays into electrons (DØ). The 95% CL contours in $\Delta\kappa$ and λ obtained from this analysis for a form factor $\Lambda = 2$ TeV are shown in Fig. 9. The axis limits are $-0.43 < \Delta\kappa < 0.59$ ($\lambda = 0$) and $-0.33 < \lambda < 0.36$ ($\Delta\kappa = 0$) for DØ, $-0.49 < \Delta\kappa < 0.54$ ($\lambda = 0$) and $-0.35 < \lambda < 0.32$ ($\Delta\kappa = 0$) for CDF, assuming again $\lambda_\gamma = \lambda_Z$ and $\Delta\kappa_\gamma = \Delta\kappa_Z$.

Because WW and WZ production is sensitive to both the WWZ and $WW\gamma$ coupling, information can be obtained on the WWZ coupling alone by setting the $WW\gamma$ coupling to its SM value. The contour limits thus obtained show that a vanishing WWZ coupling is excluded at a CL exceeding 99%. As a matter of fact, this analysis is more sensitive to the WWZ coupling than the $WW\gamma$ coupling due to the larger coupling strength of the WWZ vertex by a factor $\cot\vartheta_W$.

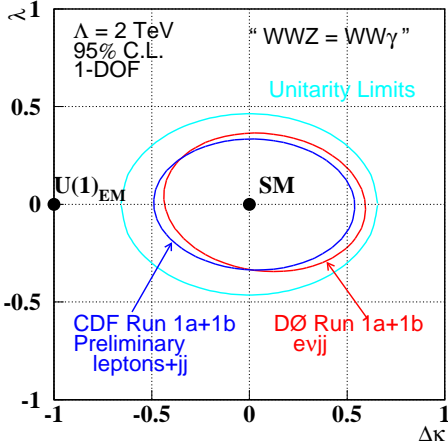


Figure 9: Contour limits on anomalous coupling parameters at the 95% CL from CDF and DØ from the analysis of WW and WZ production, using the hadronic decay of the W or Z boson, for a form factor scale of 2 TeV. The outer contour is the unitarity limit.

5.3 $W\gamma$ Production

In contrast to e^+e^- colliders where the $WW\gamma$ vertex cannot be separated from the WWZ vertex, $\bar{p}p$ colliders allow for the study of the $WW\gamma$ -vertex only, without interference from the WWZ coupling, through the study of $W\gamma$ production. In this analysis one searches for photons produced in association with a W boson. In these analyses $W\gamma$ events are selected by requiring, in addition to the regular W selection criteria, an isolated photon with high transverse energy in the central pseudo-rapidity range $|\eta_\gamma| < 1.1$ for CDF and with $|\eta_\gamma| < 1.1$ or $1.5 < |\eta_\gamma| < 2.5$ for DØ. To reduce the contribution from radiative events the photon is required to be well separated from the lepton from the W -decay.

The dominant background to this process is W +jet production with the jet being identified as a photon in the detector. For both experiments the signal to background ratio is about 3:1 with a probability of a jet “faking” a photon of about $10^{-3} - 10^{-4}$. The observed number of events are in good agreement with the number of events expected from SM processes and from the different background sources. Limits on anomalous couplings are set by performing a maximum likelihood fit to the observed p_T^γ spectrum. Based on a partial data set CDF obtained the limits: $-1.8 < \Delta\kappa < 2.0$ ($\lambda = 0$) and

$-0.7 < \lambda < 0.6$ ($\Delta\kappa = 0$). The DØ experiment has finalized the analysis using the full Run I data sample and obtains $-0.93 < \Delta\kappa < 0.94$ ($\lambda = 0$) and $-0.31 < \lambda < 0.29$ ($\Delta\kappa = 0$) [36]. Both sets of limits are obtained for a form-factor scale of $\Lambda = 1.5$ TeV (see Fig. 10).

The decay rate for $b \rightarrow s\gamma$ can also be used to set limits on anomalous couplings since the process is sensitive to photon radiation off the W -boson in the penguin diagram. The branching ratio has been measured by CLEO to be $B(b \rightarrow s\gamma) = (2.32 \pm 0.57 \pm 0.35) 10^{-4}$ [37]. The upper limit on this branching ratio excludes the outer regions in Fig. 10. The narrow region between the two allowed CLEO bands is excluded by the lower limit.

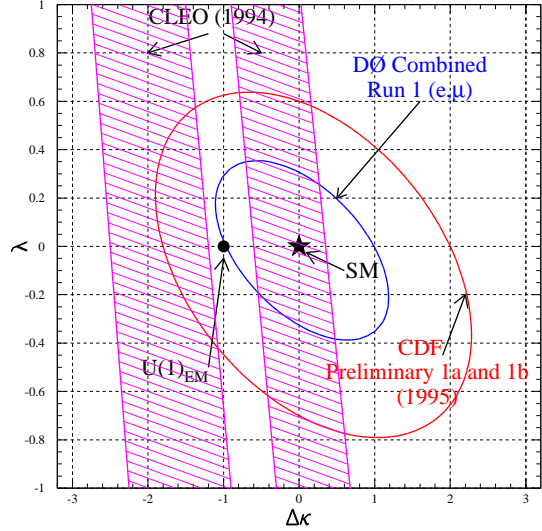


Figure 10: Limits on anomalous $WW\gamma$ couplings from $W\gamma$ analyses. The shaded bands are the constraints from CLEO.

5.4 Combined Result on $WW\gamma$ Coupling

The studies of $W\gamma$ and WW/WZ production can be combined to improve on the limits on anomalous couplings. When combining results, the correlation between the different analyses needs to be addressed. Some of the dominant common systematic uncertainties are due to the method of estimating the background and the uncertainty in structure functions and photon identification.

The DØ experiment has carried out a combined fit to the three data sets corresponding to the WW , WW/WZ and $W\gamma$ analyses based on the full Run I data. The significantly improved preliminary limits are:

$$\begin{aligned} -0.33 < \Delta\kappa < 0.45 & \quad (\lambda = 0) \\ -0.2 < \lambda < 0.2 & \quad (\Delta\kappa = 0), \end{aligned}$$

where it was assumed that the WWZ couplings and the $WW\gamma$ couplings were equal. Strong constraints are anticipated when all results from both CDF and DØ are combined.

As for the gauge boson self-interactions, again, agreement with the SM expectation is observed. But, deviations were not really expected, since most models predict anomalous couplings of order $\mathcal{O}(M_W^2/\Lambda^2)$. These measurement, however, do tell us that a W boson is more than just an electrically charged boson. The point labeled $U(1)_{EM}$ in Figs. 9 and 10 corresponds to the values of the couplings if the W boson would only couple electromagnetically. It is clear that this point is excluded by the data, showing that the W boson is really a gauge boson.

5.5 $Z\gamma$ Production

The $ZZ\gamma$ and $Z\gamma\gamma$ trilinear gauge boson couplings are described in a way analogous to the WWV couplings. These couplings, absent in the SM, are suggested by some theoretical models which imply new physics. The most general Lorentz and gauge invariant $ZV\gamma$ vertex is described by eight coupling parameters, h_i^V , ($i = 1\dots 4$), where $V = Z, \gamma$, which also are modulated by form factors to preserve unitarity, $h_i^V = h_{i0}^V/(1 + \hat{s}/\Lambda^2)^n$, where \hat{s} is the square of the invariant mass of the $Z\gamma$ system and Λ is the form-factor scale. The energy dependence of the form factor is assumed to be $n = 3$ for $h_{1,3}^V$ and $n = 4$ for $h_{2,4}^V$ [38]. Such a choice yields the same asymptotic energy behavior for all the couplings.

The study of anomalous couplings in the process $Z\gamma \rightarrow \ell\ell\gamma$ is analogous to the $W\gamma$ analysis, that is, events are selected with a photon produced in association with a Z boson and the observed number of events compared with the number of expected radiative Z and background events [39, 40]. The p_T^{γ} spectrum is again used to set limits on possible anomalous couplings.

The DØ experiment has recently performed a new analysis based on the Run Ia data, looking for

the decay $Z\gamma \rightarrow \nu\nu\gamma$ [41]. This channel has previously been studied only in e^+e^- -collisions [42, 43]. Sensitivity to anomalous couplings in this channel is much higher than in the di-lepton decay modes due to the higher decay rate into neutrinos and the absence of the radiative Z decay background. The overall background, however, is still extremely high, leading to very stringent event selection criteria. To reduce the background from W +jet events with the electron or jet being misidentified as a photon the E_T^{γ} and \cancel{E}_T were required to exceed 40 GeV. In addition, events with at least one jet with $E_T^j > 15$ GeV were rejected. The remaining background was dominated by cosmic rays and muons from beam halo which radiated in the calorimeter. This background was suppressed by rejecting events with a reconstructed muon or a minimum ionizing trace in the calorimeter close to the photon cluster. The residual background, which had roughly equal contributions from $W \rightarrow e\nu$ decays and muon bremsstrahlung, was derived from data.

Four candidate events are observed on an expected background of 5.8 ± 1.0 events and a SM prediction of 1.8 ± 0.2 events. Although the signal-to-background ratio is less than one, the sensitivity to anomalous couplings is still high, since the background is concentrated at low E_T^{γ} while the anomalous coupling contribution is almost flat in E_T^{γ} up to the kinematic threshold of the process. Limits on anomalous couplings were set at 95% CL by a fit to the E_T^{γ} spectrum and gives $|h_{30}^Z| < 0.87$, $|h_{40}^Z| < 0.21$ for $\Lambda = 500$ GeV. These limits, based on 14 pb^{-1} of data, are more stringent than the limits obtained from the analysis of the full Run I data using the electron and muon decays of the Z boson, indicating the strength of the neutrino channel. A summary of all the limits is shown in Fig. 11.

6 Conclusions

A wide variety of properties of the W and Z -bosons are now being studied at hadron colliders with ever increasing precision, at the highest energy scales achievable. All results, including the results from e^+e^- colliders [44], are in good agreement with the SM. It is widely anticipated, though, that the SM is just an approximate theory and should eventually be replaced by a more complete and fundamental description of the un-

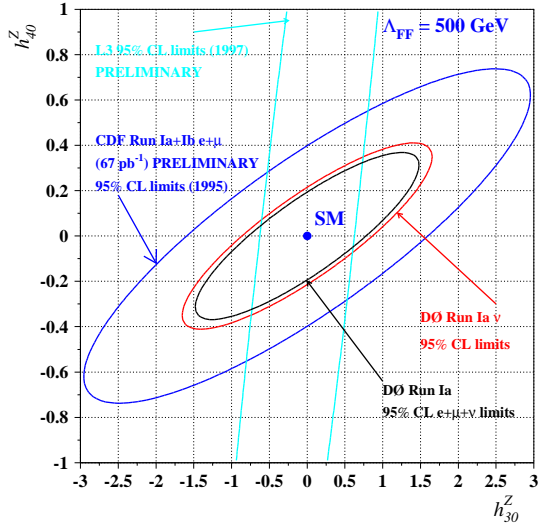


Figure 11: Limits on anomalous CP -conserving $ZZ\gamma$ couplings from $Z(\ell\ell)\gamma$ and $Z(\nu\nu)\gamma$ production for a form-factor scale $\Lambda = 500$ GeV.

derlying forces in nature. With the new data from LEP 2, SLD and the Tevatron, and with the planned upgrades of the accelerators as well as the experiments, the projected uncertainties on some fundamental parameters, especially the W mass, should provide the tools to take another ever more critical look at the SM, without any theoretical prejudice.

7 Acknowledgements

I would like to thank Debbie Errede, Bob Wagner and Darien Wood who have been very cooperative and the organizers for a very stimulating conference in a splendid setting.

1. F. Abe, *et al.* (CDF Collaboration), Phys. Rev. Lett. **73**, 220 (1994); Phys. Rev. D**52**, 2624 (1995); Phys. Rev. Lett. **76**, 3070 (1996);
S. Abachi *et al.* (DØ Collaboration), Phys. Rev. Lett. **75**, 1456 (1995).
2. R. Hamberg, W. L. van Neerven and T. Matsumura, Nucl. Phys. **B359**, 343 (1991); W. L. van Neerven and E. B. Zijlstra, Nucl. Phys. **B382**, 11 (1992).
3. H. L. Lai *et al.*, Phys. Rev. D**51**, 4763 (1995).

4. J. L. Rosner, M. P. Worah and T. Takeuchi, Phys. Rev. D**49**, 1363 (1994).
5. Particle Data Group, R.M. Barnett *et al.*, Phys. Rev. D **54**, 1 (1996).
6. C. Albajar *et al.* (UA1 Collaboration), Phys. Lett. **B253**, 503 (1991).
7. J. Alitti *et al.* (UA2 Collaboration), Phys. Lett. **B276**, 365 (1992).
8. F. Abe, *et al.* (CDF Collaboration), Phys. Rev. D**44**, 29 (1990); Phys. Rev. Lett. **69**, 28 (1992).
9. F. Abe *et al.* (CDF Collaboration), Phys. Rev. Lett. **74**, 341 (1995).
10. E. Eichten, K. Lane, M. Peskin Phys. Rev. Lett. **50** (1983) 811.
11. F. Abe *et al.* (CDF Collaboration), Phys. Rev. Lett. **67**, 2418 (1991); F. Abe *et al.*, Phys. Rev. D **49**, 1 (1994)
12. F. Abe *et al.* (CDF Collaboration), Fermilab-Pub-97/171
13. G. Alexander *et al.* (OPAL Collaboration), Phys. Lett. **B387**, 432 (1996)
14. S. Aid *et al.* (H1 Collaboration), Phys. Lett. **B353**, 578 (1995)
15. F. Abe *et al.* (CDF Collaboration), Phys. Rev. Lett. **77**, 2616 (1996).
16. J. Rosner, Phys. Rev. D **54**, 1078 (1996).
17. G. Ladinsky and C.-P. Yuan, Phys. Rev. D **50**, 4239 (1994); P.B. Arnold, R.P. Kauffman, Nucl. Phys. **B349** 381 (1991)
18. A. D. Martin, R. G. Roberts and W. J. Stirling, Phys. Lett. **B387**, 419 (1996) (1996)
19. A. D. Martin, R. G. Roberts and W. J. Stirling, Phys. Rev. D**50**, 6734 (1994)
20. E. Mirkes, Nucl. Phys. **B 387**, 3 (1992)
21. J. Alitti *et al.* (UA2 Collaboration), Phys. Lett. **B276**, 354 (1992); F. Abe *et al.* (CDF Collaboration), Phys. Rev. Lett. **65**, 2243 (1990), Phys. Rev. D **43**, 2070 (1991), Phys. Rev. Lett. **75**, 11 (1995), Phys. Rev. D**52**, 4784 (1995); S. Abachi *et al.* (DØ Collaboration), Phys. Rev. Lett. **77**, 3309 (1996).
22. W. Giele, E. Glover, D. A. Kosower, Nucl. Phys. **B403**, 663 (1993).
23. F. Abe *et al.* (CDF Collaboration), Phys. Rev. Lett. **74**, 850 (1995)
24. J. Timmermans, XVIII International Symposium on Lepton Photon Interactions, July 1997, Hamburg, Germany
25. P. Gambino and A. Sirlin, Phys. Rev. D**49**, 1160 (1994).
26. M. Shaevitz, these proceedings.
27. K. Hagiwara, R.D. Peccei, D. Zeppenfeld, K. Hikasa Nucl. Phys. **B282**, 253 (1987); K. Gaemers, G. Gounaris, Z. Phys. **C1**, 259

- (1979).
28. K. Kim and Y-S. Tsai, Phys. Rev. D **7**, 3710 (1973).
 29. CERN Report 96-01, *Physics at LEP2*, Vol.I, 525. The three parameters are related to the parameters of the effective Lagrangian through: $\Delta g_1^Z = \frac{1}{\cos^2 \vartheta_W} \alpha_{W\varphi}$, $\Delta \kappa_\gamma = -\cot^2 \vartheta_W (\Delta \kappa_Z - \Delta g_1^Z) = \alpha_{W\varphi} + \alpha_{B\varphi}$, $\lambda_\gamma = \lambda_Z = \alpha_W$.
 30. One of the rare examples where theorists reduce the number of free parameters when discussing phenomena beyond the Standard Model.
 31. K. Hagiwara, S. Ishihara, R. Szalapski, and D. Zeppenfeld, Phys. Lett. **B283**, 353 (1992), and Phys. Rev. **D48**, 2182 (1993). These so-called HISZ relations are given by $\Delta g_1^Z = \frac{1}{2 \cos^2 \vartheta_W} \Delta \kappa_\gamma$, $\Delta \kappa_Z = \frac{1}{2}(1 - \tan^2 \vartheta_W) \Delta \kappa_\gamma$, $\lambda_Z = \lambda_\gamma$.
 32. U. Baur and E.L. Berger, Phys. Rev. D **41**, 1476 (1990).
 33. F. Abe *et al.* (CDF Collaboration), Phys. Rev. Lett. **78**, 4536 (1997)
 34. F. Abe *et al.* (CDF Collaboration), Phys. Rev. Lett. **75**, 1017 (1995)
 35. S. Abachi *et al.*, Fermilab-Pub-97/136.
 36. S. Abachi *et al.* (DØ Collaboration), Phys. Rev. Lett. **78**, 3634 (1997).
 37. M.S. Alam *et al.* (CLEO Collaboration), Phys. Rev. Lett. **74**, 2885 (1995) 2885.
 38. U. Baur and E.L. Berger, Phys. Rev. **D47**, 4889 (1993).
 39. F. Abe *et al.* (CDF Collaboration), Phys. Rev. Lett. **74**, 1941 (1995)
 40. S. Abachi *et al.* (DØ Collaboration), Phys. Rev. Lett. **75**, 1028 (1995)
 41. S. Abachi *et al.* (DØ Collaboration), Phys. Rev. Lett. **78**, 3640 (1997)
 42. M. Acciarri *et al.* (L3 Collaboration), Phys. Lett. **B346**, 190 (1995).
 43. P. Abreu *et al.* (DELPHI Collaboration), Phys. Lett. **B380**, 471 (1996).
 44. D. Stickland, *these proceedings*.